Learning deficits, but normal development and tumor predisposition, in mice lacking exon 23a of *Nf1*

Rui M. Costa[1]*, Tao Yang[2,5]*, Duong P. Huynh[3], Stefan M. Pulst[3], David H. Viskochil[4], Alcino J. Silva[1] & Camilynn I. Brannan[2]

*These authors contributed equally to this work.

Neurofibromatosis type 1 (NF1) is a commonly inherited autosomal dominant disorder. Previous studies indicated that mice homozygous for a null mutation in *Nf1* exhibit mid-gestation lethality, whereas heterozygous mice have an increased predisposition to tumors and learning impairments. Here we show that mice lacking the alternatively spliced exon 23a, which modifies the GTPase-activating protein (GAP) domain of Nf1, are viable and physically normal, and do not have an increased tumor predisposition, but show specific learning impairments. Our findings have implications for the development of a treatment for the learning disabilities associated with NF1 and indicate that the GAP domain of NF1 modulates learning and memory.

Introduction

NF1 is a commonly inherited, autosomal dominant disorder that affects approximately 1 in 4,000 individuals. Mutations in the gene *NF1* cause several abnormalities in cell growth and tissue differentiation, including neurofibromas, café au lait spots and Lisch nodules of the iris[1,2]. A broad range of learning disabilities are also associated with NF1 (ref. 3). The protein encoded by *NF1*, neurofibromin, contains a GAP domain, known to inhibit Ras-mediated signal transduction[4–6]. Previous studies showed that mice homozygous for a *Nf1* null mutation exhibit mid-gestational lethality, whereas heterozygous mice have an increased tumor predisposition and learning impairments[7–9]. It is therefore unclear whether the learning disabilities are associated with developmental abnormalities or increased tumor predisposition. An alternatively spliced *NF1* exon, 23a, encodes 63 bp within the GAP-related domain. Exclusion of exon 23a results in the type I isoform, whereas inclusion of 23a results in the type II isoform. The type II isoform has a greater affinity for Ras, but lower GAP activity than type I (refs. 10,11). To determine the role of the type II isoform, we developed a mouse strain specifically lacking exon 23a (*Nf1*^{tm1Cbr}, hereafter *Nf1*$^{23a-/-}$). We found that mice homozygous for this mutation (*Nf1*$^{23a-/-}$) are viable and physically normal, and do not have an increased tumor predisposition. *Nf1*$^{23a-/-}$ mice, however, have specific learning impairments in hippocampal-dependent tasks (water maze and contextual discrimination) similar to those previously described for heterozygous null mutants[9]. These results demonstrate that the *Nf1* type II isoform is not required for either normal embryological development or tumor suppression, but is essential for normal brain function. Also, they indicate that the GAP-related domain of neurofibromin modulates learning and memory.

Results

Mice lacking exon 23a are viable and lack Nf1 type II

We made the exon 23a deletion vector by joining a DNA fragment located upstream of *Nf1* exon 23a to a fragment 3′ of exon 23a, generating a deletion of approximately 300 bp that included exon 23a (Fig. 1*a*). For positive selection of the targeting vector, a neomycin resistance cassette previously shown not to affect the transcription or splicing of the surrounding exons[12] was inserted in the deletion. After electroporation of the targeting vector and subsequent selection and screening of embryonic stem (ES) cell clones, 19 independent clones were identified that had the expected deletion of exon 23a.

Male chimeric mice were generated from two independent exon 23a deletion ES cell lines using standard procedures[13]. Upon maturity, males derived from each cell line were mated with C57BL/6J females, and germline transmission of the exon 23a deletion mutation was obtained from both lines. The resulting F_1 progeny were intercrossed to obtain F_2 mice of all three genotypes in the expected mendelian ratio. These (C57BL/6J×129/SvEv) F_2 animals were used in the experiments described below. Identical results were obtained from both independent lines; therefore, we combined them.

To confirm that the engineered mutation resulted in deletion of exon 23a, we used RT–PCR from RNA derived from brain tissue. We determined that the type II isoform was missing from *Nf1*$^{23a-/-}$ animals, but present in *Nf1*$^{23a+/+}$ and *Nf1*$^{23a+/-}$ animals (Fig. 1*b*). Moreover, *Nf1*$^{23a-/-}$ animals seemed to have normal levels of the type I isoform, indicating that the intronic neomycin resistance gene had no adverse affect on *Nf1* expression. Protein extracts prepared from brain tissue were analyzed by western-blot analysis using two affinity-purified

[1]*Departments of Neurobiology, Psychiatry and Psychology, BRI, UCLA, Los Angeles, California, USA.* [2]*Department of Molecular Genetics and Microbiology, Center for Mammalian Genetics, and the University of Florida Brain Institute, University of Florida College of Medicine, Gainesville, Florida, USA.* [3]*Cedars-Sinai Medical Center, UCLA School of Medicine, Los Angeles, California, USA.* [4]*Division of Medical Genetics, University of Utah, Salt Lake City, Utah, USA.* [5]*Present address: Brigham and Woman's Hospital, Boston, Massachusetts, USA. Correspondence should be addressed to A.J.S. (e-mail: Silvaa@mednet.ucla.edu) or C.I.B. (e-mail: Brannan@mgm.ufl.edu).*

anti-neurofibromin peptide antibodies[14]: NF1C, which recognizes the C terminus of neurofibromin; and GAP4, which recognizes the 21 amino acids encoded by exon 23a. We determined that, although all three genotypes express type I neurofibromin, only $Nf1^{23a+/+}$ and $Nf1^{23a+/-}$ mice express type II (Fig. 1*c*). These data demonstrate that the targeted deletion of *Nf1* exon 23a results in loss of type II neurofibromin. We then performed immunohistochemical analysis of brain tissue with the GAP4 antibody using $Nf1^{23a-/-}$ tissue as a negative control for antibody specificity. In contrast to previous studies using RT–PCR analysis of mouse cortical cultures[15], we found that type II neurofibromin is not only expressed in glia, but also in mature neurons in the mouse adult brain, including pyramidal neurons in the CA3 region of the hippocampus, Purkinje and granule cells in the cerebellum (Fig. 1*d–i*).

$Nf1^{23a-/-}$ mice do not have increased predisposition for tumor formation

We analyzed 28 adult mice (between the ages of 4 and 13 months; average 8 months) at the histopathological level (13 $Nf1^{23a-/-}$, 10 $Nf1^{23a+/-}$ and 5 $Nf1^{23a+/+}$). Complete examination revealed that only 4 of 28 mice had any abnormalities, but no abnormality was found more than once. One male $Nf1^{23a-/-}$ mouse (8 months) had an enlarged spleen (6 times normal) containing splenic hyperplasia with expansion of red pulp and increased extramedullar hematopoiesis. The lung, liver and kidneys revealed mild interstitial lymphocyte infiltrates. Another $Nf1^{23a-/-}$ male (13 months) had a small liver adenoma (0.3 cm) and a small lung adenoma (0.3 cm). A $Nf1^{23a-/-}$ female mouse (9 months) contained a large intra-abdominal cyst filled with yellow serous fluid. Microscopic examination revealed features consistent with endometriosis. Finally, a $Nf1^{23a+/-}$ male (6.5 months) had an enlarged kidney (2 times normal), which on sectioning revealed multiple cystic lesions in the medulla and seemed to be a renal cystadenoma. The remaining 24 mice were found to be completely normal, indicating that there are neither obvious genotype-associated pathologies nor an increased risk for malignancy within the first year of life.

Examination of brain sections from all 28 mice stained with hematoxylin and eosin revealed no gross or microscopic abnormalities among the three genotypes. As there have been reports of astrogliosis in individuals with NF1 and in $Nf1^{+/-}$ mice[16,17], we investigated the distribution of astrocytes in the brain by immunostaining with glial fibrillary acid protein (GFAP) antibody. Overall, no differences in the GFAP staining pattern or intensity were seen among the three groups of mice (data not shown).

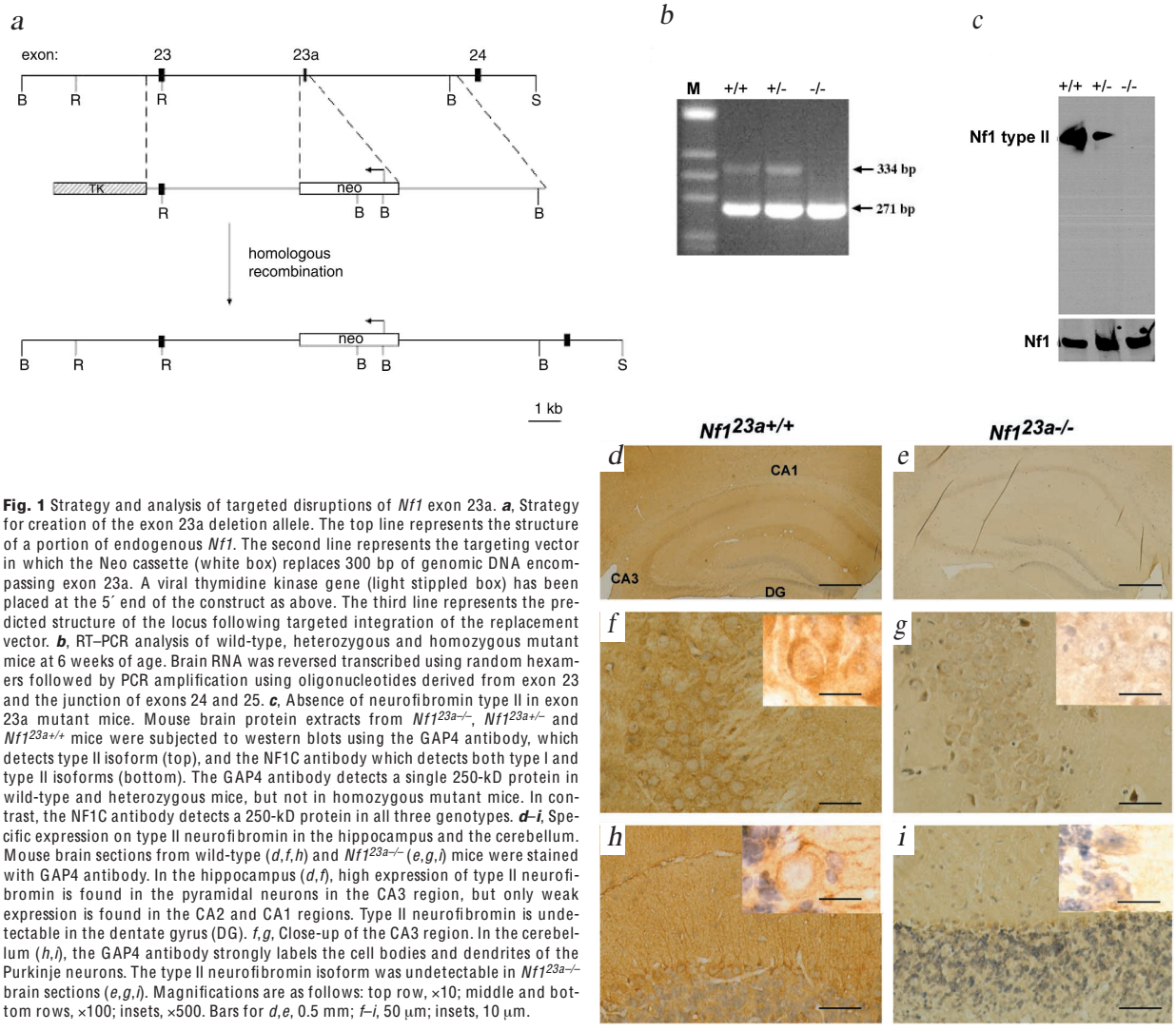

Fig. 1 Strategy and analysis of targeted disruptions of *Nf1* exon 23a. ***a***, Strategy for creation of the exon 23a deletion allele. The top line represents the structure of a portion of endogenous *Nf1*. The second line represents the targeting vector in which the Neo cassette (white box) replaces 300 bp of genomic DNA encompassing exon 23a. A viral thymidine kinase gene (light stippled box) has been placed at the 5′ end of the construct as above. The third line represents the predicted structure of the locus following targeted integration of the replacement vector. ***b***, RT–PCR analysis of wild-type, heterozygous and homozygous mutant mice at 6 weeks of age. Brain RNA was reversed transcribed using random hexamers followed by PCR amplification using oligonucleotides derived from exon 23 and the junction of exons 24 and 25. ***c***, Absence of neurofibromin type II in exon 23a mutant mice. Mouse brain protein extracts from $Nf1^{23a-/-}$, $Nf1^{23a+/-}$ and $Nf1^{23a+/+}$ mice were subjected to western blots using the GAP4 antibody, which detects type II isoform (top), and the NF1C antibody which detects both type I and type II isoforms (bottom). The GAP4 antibody detects a single 250-kD protein in wild-type and heterozygous mice, but not in homozygous mutant mice. In contrast, the NF1C antibody detects a 250-kD protein in all three genotypes. ***d–i***, Specific expression on type II neurofibromin in the hippocampus and the cerebellum. Mouse brain sections from wild-type (*d,f,h*) and $Nf1^{23a-/-}$ (*e,g,i*) mice were stained with GAP4 antibody. In the hippocampus (*d,f*), high expression of type II neurofibromin is found in the pyramidal neurons in the CA3 region, but only weak expression is found in the CA2 and CA1 regions. Type II neurofibromin is undetectable in the dentate gyrus (DG). *f,g*, Close-up of the CA3 region. In the cerebellum (*h,i*), the GAP4 antibody strongly labels the cell bodies and dendrites of the Purkinje neurons. The type II neurofibromin isoform was undetectable in $Nf1^{23a-/-}$ brain sections (*e,g,i*). Magnifications are as follows: top row, ×10; middle and bottom rows, ×100; insets, ×500. Bars for *d,e*, 0.5 mm; *f–i*, 50 μm; insets, 10 μm.

Because the *Nf1*$^{+/-}$ mice have increased predisposition for tumor formation and lower survival rates than wild-type controls[8], we aged another cohort of 27 mice (9 wild type, 10 *Nf1*$^{23a+/-}$, 8 *Nf1*$^{23a-/-}$) for over two years and analyzed their survival rates at different ages. No differences were observed in the survival rates of the different genotypes (Table 1; χ^2_6=2.27, P>0.05). At the age of 27 months, the surviving mice were euthanized and necropsy was performed. One wild-type female had pus in the abdominal cavity with enlarged spleen and one *Nf1*$^{23a-/-}$ male had a large (0.5 cm), well-confined mass in the prostate area, but no consistent pathology was seen among the three genotypes.

Table 1 • Survival rates of the different genotypes

Age (months)	12	18	24	27
Genotype				
wild type	100%	77%	77%	44%
Nf1$^{23a+/-}$	100%	100%	90%	50%
Nf1$^{23a-/-}$	100%	87.5%	75%	50%

We aged 27 mice (9 wild type, 10 *Nf1*$^{23a+/-}$ and 8 *Nf1*$^{23a-/-}$) to 27 months and analyzed their survival rates at different ages. No differences were observed in the survival rates of the different genotypes (χ^2_6=2.27, P>0.05).

Spatial learning is impaired in *Nf1*$^{23a-/-}$ mice

Visual-spatial problems are among the most common cognitive deficits detected in NF1 patients[3] and previous results showed that *Nf1*$^{+/-}$ mice have abnormal spatial learning[9]. To determine whether the *Nf1*$^{23a-/-}$ mutation affected spatial learning, we tested these mice in the hidden version of the water maze, a task known to be sensitive to hippocampal lesions[18]. In this task an animal learns to locate a submerged platform in a pool filled with opaque water. During training, mice were given 2 trials per day for 14 days. No differences were observed between wild-type and mutant mice in floating, thigmotaxic behavior or swimming speed (wild type=19.9 cm/s, mutants=18.9, $F_{1,22}$=0.297, P>0.05). Across days, all animals decreased the time taken to find the platform ($F_{1,21}$=13.914, P<0.05) and no difference was found between *Nf1*$^{23a-/-}$ mice and wild-type littermates ($F_{1,21}$=2.548, P>0.05; Fig. 2*a*). The time taken to find the platform during training is known to be a poor measure of spatial learning[19]. Therefore, we assessed spatial learning in probe trials in which the platform was removed from the pool. In a probe trial given after 10 days of training, the wild-type mice searched selectively, spending significantly more time searching for the platform in the quadrant where the platform was during training than in the other quadrants ($F_{3,44}$=12.242, P<0.05), whereas *Nf1*$^{23a-/-}$ mice searched randomly ($F_{3,44}$=2.716, P>0.05) and spent significantly less time searching for the platform in the training quadrant than wild type ($F_{3,22}$=6.555, P<0.05; Fig. 2*c*). Using another very sensitive measure to assess spatial learning[20] (proximity to platform), we verified that wild-type mice searched on average closer to the exact platform position than to the symmetrically opposite position in the pool (t_{11}=–2.612, P<0.05), whereas mutants did not (t_{11}=0.709, P>0.05; Fig. 2*e*).

Previous studies showed that additional training alleviates the learning deficits in the *Nf1*$^{+/-}$ mice[9]. Consistently, following four additional days of training, the *Nf1*$^{23a-/-}$ mice searched as selectively as wild-type controls in a probe test (F=1.301, P>0.05; Fig. 3*d*). They spent significantly more time searching in the training quadrant than in the other quadrants ($F_{3,44}$=15.348, P<0.05) and searched closer to the exact platform position (t_{11}=–2.905, P<0.05; Fig. 3*f*).

To determine whether deficits in motivation, motor coordination, or vision account for the abnormalities in spatial learning,

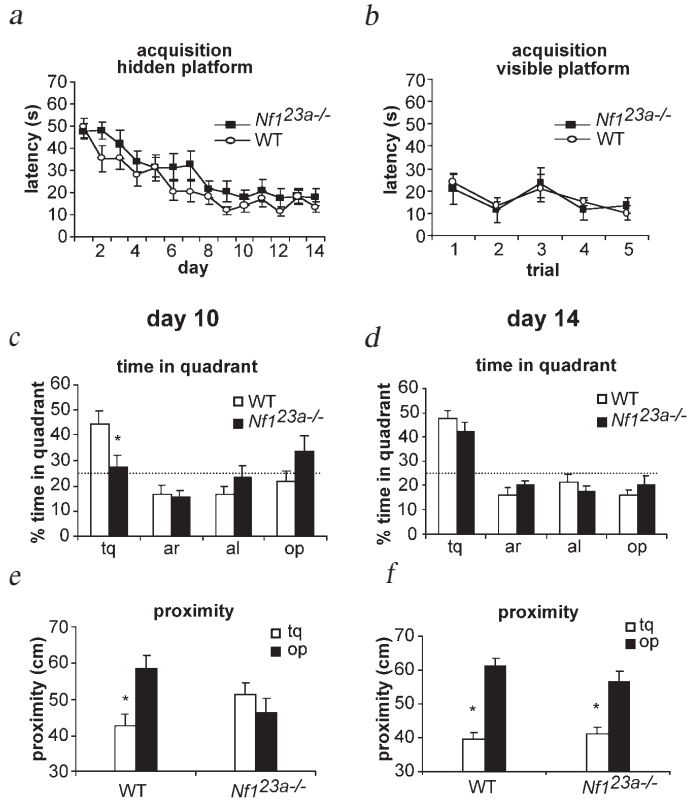

Fig. 2 Spatial learning in the water maze. ***a***, *Nf1*$^{23a-/-}$ mice (n=12) and wild-type littermates (n=12) were trained for 14 d, with 2 trials per day in the water maze. The average latency to reach the hidden platform is plotted. Escape latencies decrease across days ($F_{1,21}$=13.914, P<0.05) and there is no difference in latencies between mutants and controls during training ($F_{1,21}$=2.548, P>0.05). ***b***, After the hidden version of the water maze, the animals were run in the visible platform task. There was no difference in latency to get to the platform across trials between wild-type and mutants ($F_{1,14}$=0.30, P>0.05). ***c***, Results of a probe trial given after 10 days of training. The percentage of time animals spent searching in each of the training quadrants is shown. ANOVA shows that there is an effect of percentage time spent in quadrant for wild type ($F_{3,44}$=12.242, P<0.05). Post-hoc analysis show that wild-type mice spent significantly more time searching in the training quadrant than in any of the other quadrants (Fisher PLSD, P<0.05). Mutants did not search selectively in any of the quadrants ($F_{3,44}$=2.716, P>0.05) and spent significantly less time searching in the training quadrant than wild type ($F_{1,22}$=6.555, P<0.05). ***d***, Probe trial given after 14 days of training. Both mutants ($F_{3,44}$=15.348, P<0.05) and wild type ($F_{3,44}$=23.110, p<0.05) searched selectively and spent significantly more time searching in the training quadrant than in any of the other quadrants (Fisher PLSD, P<0.05). ***e***, During the probe trial given at day 10, wild-type mice searched on average closer to the exact position of the platform during training than to the symmetric position in the opposite quadrant (t_{11}=–2.612, P<0.05), whereas mutants did not (t_{11}=0.709, P>0.05). ***f***, Probe trial day 14. Both mutants and wild type searched on average closer to the exact platform position than to the opposite position in the pool (t_{11}=–2.905, P<0.05; t_{11}=–6.71, P<0.05). Dashed line indicates random search (25% in each quadrant). *Significant difference, P<0.05. tq, training quadrant; ar, adjacent right quadrant; al, adjacent left quadrant; op, opposite quadrant.

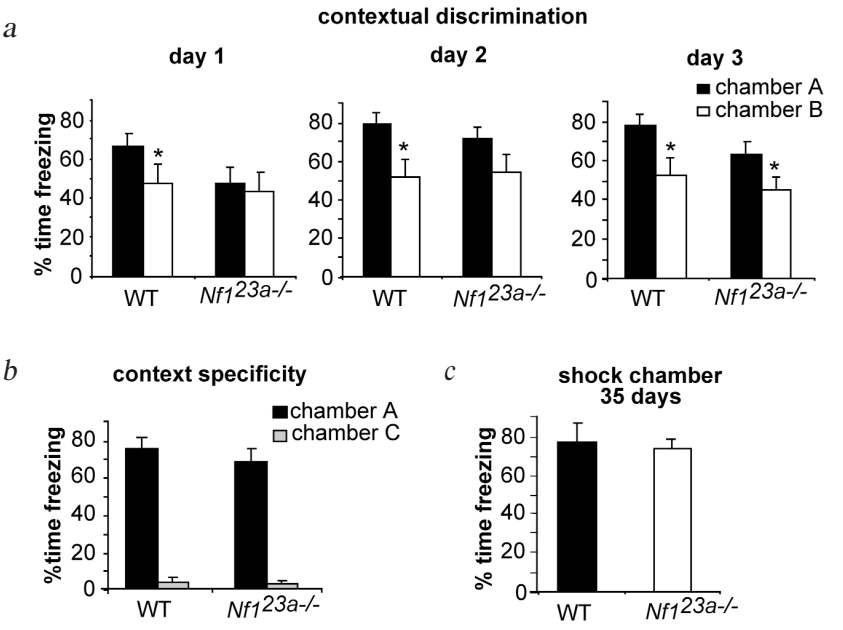

Fig. 3 Contextual discrimination. ***a***, Percentage of time spent freezing in chamber A (shock context, filled) versus chamber B (no-shock context, open bars) shown for each of the three testing days. Wild-type mice spent significantly more time freezing in the chamber where they were shocked than in the other chamber on each test day (day 1, A=66.8, B=47.4, t_8=2.407, P<0.05; day 2 A=78.0, B=51.2, t_8=5.873, P<0.05; day 3, A=77.2, B=52.2, t_8=4.890, P<0.05), showing that they discriminate between the two chambers. *Nf1*$^{23a-/-}$ mutants did not discriminate between the chambers (day 1, A=47.5, B=43.3, t_8=0.603, P>0.05; day 2, A=70.5 B=53.5, t_8=1.839, P>0.05) during the first two days of training, but they finally discriminated after three days of training (A=62.4, B=44.8, t_8=2.534, P<0.05). ***b***, Specificity of the conditioned freezing. After training in contexts A and B, mutants and wild-type mice were tested in chamber A and a novel chamber, C. Both mutants (A=66.6, C=3.1) and wild-type (A=73.7,C=3.8) showed similarly robust freezing in chamber A (shock context, black bars, $F_{1,15}$=0.637, P>0.05) and essentially no freezing in chamber C (novel context, gray bars, $F_{1,15}$=0.111, P>0.05). ***c***, Memory consolidation does not seem to be impaired in the mutants because both mutant (open bars) and wild-type controls (filled bars) exhibited similar levels of freezing (wild type=77.1, mutants=73.5, $F_{1,15}$=0.111, P>0.05) when re-exposed 35 days later to the same chamber where they were shocked. *Significant difference, P<0.05.

the same animals were tested in the visible platform version of the water maze, a task that is not affected by hippocampal lesions[18]. In this task, animals must locate a platform marked with a visible cue. Both mutant and wild-type control mice acquired the task similarly, as the times taken to reach the visible platform were not different between the groups ($F_{1,14}$=0.030, P>0.05, Fig. 3*b*).

Nf1$^{23a-/-}$ mice are impaired in contextual discrimination

We confirmed the water maze results using another hippocampal-dependent task, contextual discrimination[21]. In this task animals are required to discriminate between two similar chambers, one in which they receive a mild foot shock (chamber A) and another in which they do not (chamber B). Contextual discrimination is assessed by measuring the time spent 'freezing' (that is, without any bodily movement aside from respiration) in each chamber. Throughout training, wild-type mice froze significantly more in the chamber where they were shocked than in the other chamber (P<0.05 for all three days), showing that they discriminate between the two chambers (Fig. 3*a*). In contrast, during the first two days of training, *Nf1*$^{23a-/-}$ mutants did not discriminate between the chambers (P>0.05 for both days). *Nf1*$^{23a-/-}$ mice finally discriminated between the chambers after three days of training (day 3, t_8=–2.534, P<0.05), confirming that, just as with spatial learning, additional training can overcome the learning deficits. When tested in chamber C, which is very different from the training chambers, both wild-type and mutant mice showed little or no freezing (Fig. 3*b*). This demonstrates that the freezing responses in chamber B are probably triggered by the cues shared with chamber A. The *Nf1*$^{23a-/-}$ mutation does not seem to affect long-term memory, because mutants and controls had similar levels of freezing ($F_{1,15}$=0.111, P>0.05) when tested 35 days after training (Fig. 3*c*). Also, the ability to freeze seems to be unaffected by the mutation. In chamber A, both baseline freezing (wild type, 9.0; *Nf1*$^{23a-/-}$, 6.7; $F_{1,15}$=0.264, P>0.05) and freezing after foot-shock delivery ($F_{1,15}$=3.495, P>0.05) were similar between wild type and mutants.

Nf1$^{23a-/-}$ mice have delayed acquisition of motor skills

Some individuals with NF1 show delayed acquisition of motor skills and motor coordination problems[3]. To determine whether the *Nf1*$^{23a-/-}$ mutation affects motor function, we tested the mice on an accelerating rota-rod[22,23] (4–40 r.p.m. in 300 s). *Nf1*$^{23a-/-}$ mice fell off the rotating rod sooner than wild-type mice ($F_{1,17}$=4.84, P<0.05; Fig. 4*a*). This motor coordination impairment is not due to greater fatigue in the mutants because, at an intermediate, constant speed (14 r.p.m), mutants and controls showed no differences in latency to fall from the rotating rod ($F_{1,16}$=0.262, P>0.05; Fig. 4*b*).

The effects of the *Nf1*$^{23a-/-}$ mutation are specific

It is unlikely that the learning deficits in these mice are caused by generalized neurological problems or poor motor performance, as swimming speed, ability to freeze, ambulance (hind paw analysis[23]), exploratory behavior (open field[23]), muscular strength (wire hang[24]) and body weight (data not shown) were not affected by the mutation.

Just as NF1 patients do not show learning deficits in all tasks, the *Nf1*$^{23a-/-}$ mutation did not affect all forms of learning. When tested in the social transmission of food preferences[25], a task that assesses the capability of an animal to remember a food smelled in the breath of a littermate, *Nf1*$^{23a-/-}$ mice learned as well as wild-type controls (t_8=3.23, P<0.05; Fig. 5). This is relevant because the brain regions required to solve this task[26] are different from the ones required for the water maze[18] and contextual discrimination[21], revealing that the effects of this mutation are specific.

Discussion

Neurofibromin is a complex protein that is implicated in a number of biological processes, including growth, differentiation, learning and memory. Accordingly, inactivating mutations of *NF1* in humans and mice results in a wide spectrum of symptoms ranging from increased tumor predisposition to learning disabilities[27]. *NF1* encodes several distinct isoforms of neurofibromin.

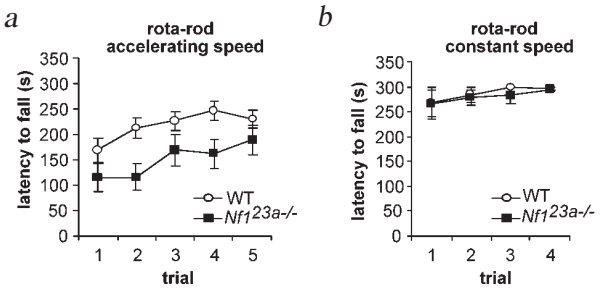

Fig. 4 Motor performance in the rota-rod. ***a***, Accelerating rota-rod. Wild-type and *Nf1*$^{23a-/-}$ were given 5 trials in an accelerating rota-rod (4–40 r.p.m. in 5 min) during 1 day. All subjects showed an increase in the latency to fall across trials ($F_{1,17}$=13.3, P<0.05) indicating that they improved their performance across trials. In average mutants fell off the rotating rod sooner than the wild type ($F_{1,17}$=4.84, P<0.05). ***b***, Constant speed rota-rod. The mice were given four trials at a lower constant speed (14 r.p.m. for 5 min) during one day. Under these conditions, mutants and controls showed no differences in latency to fall from the rotating rod ($F_{1,16}$=0.262, P>0.05).

Here we have demonstrated that one isoform, type II, is important for brain function, but not for embryological development or tumor suppression. It is possible that other alternatively spliced exons (such as exon 9a) expressed postnatally in forebrain neurons[28], also have a role in mechanisms underlying learning and memory. Our data indicate that the learning deficits caused by mutations that inactivate *NF1* in mice and humans are not a result of developmental deficits or undetected tumors. Instead, they suggest that the learning deficits in individuals with NF1 are caused by the disruption of neurofibromin function in the adult brain, a finding with important implications for the development of a treatment for the learning disabilities associated with NF1.

Exon 23a modifies the GAP domain of NF1. Thus, our results indicate that modulation of the Ras pathway is important to learning and memory. These data are consistent with previous findings. First, patients carrying a missense mutation that specifically eliminates the Ras-GAP activity of neurofibromin have learning disabilities[29]. Second, pharmacological disruption of the downstream Ras target MAPK disrupts learning in rodents[30]. Third, a deletion mutation of Ras guanine-nucleotide-exchange factor (Ras-GRF) also affects learning and memory in mice[31]. In addition, *Nf1*-null mutations are known to elevate Ras-GTP (refs. 32,33), and cause learning disabilities[9]. These results suggest that either abnormally high or low Ras-GTP levels affect learning and memory. It has been shown that type I neurofibromin has higher GAP activity and lower affinity for Ras than type II (refs. 10,11), offering the possibility that the ratio between the two isoforms modulates Ras signaling. Because *Nf1* type I and type II isoforms are expressed in some of the same populations of cells in the adult brain, and the relative expression of these two isoforms in neuronal cultures is subject to modulation by extrinsic factors, such as NGF (ref. 34), we propose that differential expression of these two isoforms may have a role in fine-tuning Ras activity in the central nervous system.

Although the neurological and cognitive deficits associated with NF1 are pleiomorphic and incompletely penetrant (only about half of individuals show learning disabilities), spatial problems are the most common abnormality associated with this condition. Although it is unclear whether the same brain systems underlie the spatial phenotype in mice and humans, it is important to note that both the heterozygous null *Nf1* mutation and the *Nf1*$^{23a-/-}$ mutation primarily result in incompletely penetrant spatial learning deficits in mice. Additionally, *NF1* mutations can result in motor coordination problems in both mice and humans. These compelling parallels demonstrate the usefulness of mouse models to understand the etiology of learning deficits in NF1.

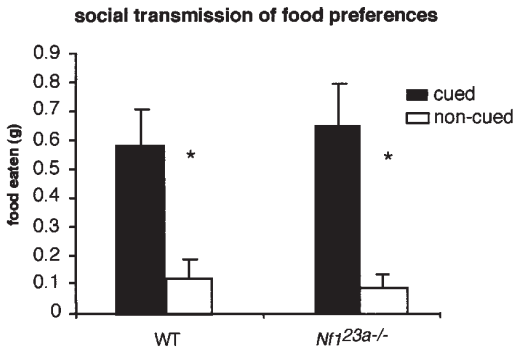

Fig. 5 Social transmission of food preferences. After 15 min of interaction with demonstrator mice, both wild-type and mutant mice showed robust socially transmitted food preference (wild type, cued=0.58 g, non-cued=0.12 g, t_8=3.16, P<0.05; *Nf1*$^{23a-/-}$, cued=0.65 g, non-cued=0.09 g, t_8=3.23, P<0.05). Even with shorter interaction times (5 min), no differences were observed between mutant and wild-type mice (data not shown).

Methods

Targeted deletion of exon 23a. The exon 23a deletion vector was made by joining a 5′ upstream 4.8 kb *Bsr*FI fragment containing exon 23 to a 3′ downstream 4.6 kb *Bst*BI-(*Not*I) fragment containing intronic sequence. This resulted in a deletion of approximately 300 bp of genomic DNA, which included exon 23a. A neomycin selectable marker (KT3NP4) was inserted between the two fragments in the opposite transcriptional orientation relative to *Nf1* and a PGK-TK cassette was placed at the 5′ end of the construct. CJ.7 cells[35] were cultured and electroporated with linearized vector using standard conditions[36], and then plated onto gelatin coated dishes in media containing ESGRO (1,000 μ/ml; Gibco BRL). After 24 h, the culture medium was changed to include 250 μg/ml active concentration of Geneticin (Gibco BRL). After 48 h it was changed again to include 0.7 μM FIAU (0.7 μM; Oclassen Pharmaceuticals). Seven days after electroporation, 500 Geneticin- and FIAU-resistant colonies were picked and expanded on mouse embryo fibroblasts in the presence of Geneticin. We isolated genomic DNA from ES cells as described[37]. Aliquots of the DNA (5 μg) were digested to completion with *Bam*HI, then electrophoresed through 0.8% agarose gels, transferred to Hybond nylon membranes (Amersham) and subsequently screened using a 0.5-kb *Eco*RI-*Spe*I fragment mapping 5′ to the limit of homology. Autoradiography was carried out at –70 °C using Kodak XAR film. We found the expected replacement event in 1 of every 9 clones. We selected two independent clones to derive chimeric mice according to standard procedures[13].

RT–PCR. We pretreated total brain RNA (10 μg) with DNase I (Gibco BRL). Half of the reaction was subsequently used to synthesize first-strand cDNA with Superscript II reverse transcriptase (Gibco BRL) and random primers (Gibco BRL). The other half of the reaction was manipulated in parallel in the absence of RT. We used one-twentieth of the +RT or –RT reactions to program PCR reactions using the following conditions: 10 mM Tris-HCl, pH 8.3, 50 mM KCl, 1.5 mM $MgCl_2$, 0.125 mM of the four dNTPs, 1 unit *Taq* DNA polymerase (Boehringer) and 4 μM each of the primers 5′–GCGGAACCTCCTTCAGATGACTG–3′ and 5′–GCTCTGAAGTACCTTTGAC–3′. PCR amplification conditions were as follows: 95 °C for 4 min, followed by 40 cycles of 94 °C for 1 min, 55 °C for 1 min, and 72 °C for 2 min. The final cycle was followed by a 10-min extension period at 72 °C.

Genotyping. To genotype genomic DNA isolated from the exon 23a deletion mice, we used three oligonucleotide primers: Nf23a,

5′–GCAACTTGCCACTCCCTACTGAATAAAGCTACAGTAAAA–3′; intron 23a, 5′–CCACTCACATGACCCGCAAACG–3′; and KT3NP4, 5′–GGAGTTGTTGACGCTAGGGCTC–3′. PCR conditions were the same as above except of the following changes: 25 µl reactions were used containing 400 ng each of the 3 oligonucleotide primer. PCR of DNA from wild-type animals resulted in a 450-bp fragment; from homozygous mutant animals, a 520-bp fragment; and from heterozygous animals, both a 450-bp and a 520-bp fragment.

Western blot. Mouse brains were homogenized in triple detergent buffer (100 mM Tris-HCl, pH 8.0, 150 mM NaCl, 1% Triton X-100, 0.5 mM deoxycholic acid, 1% SDS, 50 ng/ml Pefabloc, 2 U/ml aprotinin, 1 mM EGTA, 2 µg/ml pepstatin) and spun for 1 h at 100,000*g* at 4 ºC. Protein concentration was determined using the Bradford Protein Detection kit (Biorad). Western blots were performed on the same day of protein extraction by first precipitating protein extracts (100 µg) with acetone, which was then dissolved in 1×SDS–PAGE sample buffer and run on a 4–20% premade SDS–PAGE (Biorad) for 1 h. Proteins were then transferred to Amersham nitrocellulose filter overnight at 4 ºC in western-blot buffer. The filters were then probed with either GAP4 or NF1C antibodies (1 µg/ml) using a chemiluminescent kit according to manufacturer's instructions (Amersham). Both GAP4 and NF1C were previously characterized[14].

Pathology. Age- and sex-matched adult mice were killed and internal organs removed for analysis. After gross examination, the tissues were fixed in 10% neutral buffered formalin. Representative tissue sections were dehydrated, embedded in paraffin, sectioned (5 µm), mounted on slides and stained with hematoxylin and eosin.

Imunohistochemistry. For the GAP4 antibody imunohistochemistry, the mice were infused through the heart with DPBS, followed by 2% paraformaldehyde in DPBS. The brains were then removed and processed for paraffin embedding. We cut 5-µm sections. Sections were boiled in sodium citrate (10 mM, pH 6) for 10 min to unmask the GAP4 antigenic site, blocked with avidin/biotin and 3% normal goat serum. Sections were then incubated with affinity-purified GAP4 antibody[14] overnight at 4 ºC. Primary antibodies were detected using the Vector rabbit ABC elite Peroxidase kit (Vector), enhanced by DAB enhancer, and visualized with diaminobenzidine (DAB) (Biomedia). The sections were then counterstained with aqueous hematoxylin (Xymed). The same basic procedure was used for GFAP staining using an automated immunohistochemistry stainer (Ventana Medical System 320, and rabbit anti-cow GFAP antibody (Dakopatts) at 1:1,200 dilution as a primary antibody.

Animals. For the behavioral experiments, we used group-housed males and females. The experimenters were blind to the genotype of each animal during the experiments. All the protocols used were approved by UCLA's Animal Research Committee.

Water maze. The basic protocol for the water maze experiments has been described[38]. Our pool is circular with a 1.2-m diameter and the platform has an 11-cm diameter. The water is made opaque with non-toxic white paint and maintained at 27 ºC. The movement of the mice is processed by a digital tracking device (VP118, HVS Image). During the hidden platform test, the platform was submerged (1 cm) below the water surface and maintained in the same place throughout training. The mice were given 2 trials every day (60 s ITI) for 14 d and the starting position was varied from trial to trial. In the probe trials given after 10 and 14 d of training, the platform was removed and the mice were allowed to search for it for 60 s. In the visible platform test, a distinct symmetrical cue (black and white golf ball) was fixed 5 cm above the center of the submerged platform. The animals were given 5 trials during 1 day (30 min ITI); the starting position and the platform location were pseudo-randomly varied from trial to trial.

Contextual discrimination. The contextual discrimination experiments were performed as described[21]. Chambers A and B were similar, both with grid floors and located in sound attenuating boxes in dimly lit rooms located outside the vivarium; and they were modified to have some unique features (location, geometry, background noise, odor). Chamber C, which shared no obvious cues with chambers A and B, was located in a room inside the mouse vivarium and was brightly illuminated. This experiment consisted of three stages: pre-exposure (1 d), training (1 d) and testing (3 d). Each mouse was habituated to contexts A and B for 10 min before training started (day –1). The next day (day 0) animals were placed in chambers A and B for 3 min (the order was balanced), and after 150 s a mild foot-shock (0.75 mA for 2 s) was delivered in chamber A but not in chamber B. During the 3 consecutive testing days animals were placed in each chamber and the amount of freezing during the initial 150 s was measured. Freezing was assessed every 5 s: mice were scored as freezing if they were immobile (cessation of all bodily movement aside from respiration) for 2 s. On each of the testing days animals were shocked after 150 s in chamber A but not in chamber B. Context specificity was tested 24 h after the end of the contextual discrimination task by placing the animals in chambers A and C and measuring the amount of freezing. Long-term memory was assessed 35 d after the end of the contextual discrimination task.

Rota-rod. For the accelerating rota-rod task using a rota-rod (Ugo Basile 7650) accelerating from 4 to 40 r.p.m. in 300 s. 5 trials (35 min ITI) during the same day were given. For the constant speed rota-rod task, animals were given 4 trials (5 min) during the same day, with the rota-rod rotating at 14 r.p.m. The latency for the animals to fall from the rota-rod was measured. If the mice initiated passive rotation (that is, grabbed the rotating rod with all four paws and avoid falling) that was considered a fall.

Social transmission of food preferences. This task was performed as described[25,26]. Mice were shaped to eat ground chow from a metal cup. First, a demonstrator mouse was removed from each cage and food deprived for 24 h. The demonstrator mouse was then allowed to eat scented food for 1 h and placed back in the cage for a period of 15 min to interact with the other mice in the cage (observers). After this, observers were food-deprived for 24 h. Finally, observer mice were tested for their preference in a 1-h test in which they had a choice between the food they smelled on the demonstrator's breath and another scented food. The amount of each food eaten (g) was measured. The demonstrated scents were pseudo-randomly assigned to each cage of mice.

Statistical analysis. A two-way ANOVA with repeated measures was used to analyze the acquisition data from the water maze and rota-rod tasks. To analyze the performance in the water maze probe trials we used a single-factor ANOVA on the percentage time in quadrant; post-hoc comparisons between quadrants were performed when there was an effect of quadrant. Planned comparisons using a paired *t*-test were used to analyze the contextual discrimination data, the proximity data in the water maze and the social transmission of food preference data.

Acknowledgments

We thank K. Thomas for the KT3NP4 neomycin cassette; R. White for support in the generation of the GAP4 antibody; D.H. Gutmann for help interpreting the immunohistochemistry; P.W. Frankland for discussions; and C.M. Spivak for inspiration and support. R.C.M. is supported by the GABBA Graduate Program (Oporto University) and the Portuguese Foundation for Science and Technology (BD 13854/97). This work was supported by a grant from the Department of Defense, U.S. Army Medical Research and Materiel Command (DAMD17-97-1-7339) to C.I.B.; grants from the NIH (R01 NS38480), the Neurofibromatosis Consortium and the Neurofibromatosis Foundation to A.J.S.; and a donation from C.M. Spivak to A.J.S.

Received 11 December 2000; accepted 26 January 2001.

1. Gutmann, D.H. & Collins, F.S. von Recklinghausen neurofibromatosis. *The Metabolic and Molecular Basis of Inherited Disease* 1–19 (McGraw Hill, New York, 1994).
2. Huson, S.M. & Hughes, R.A.C. *The Neurofibromatoses: A Pathogenic and Clinical Overview* (Chapman & Hall, London, 1994).
3. Ozonoff, S. Cognitive impairment in neurofibromatosis type 1. *Am. J. Med. Genet.* **89**, 45–52 (1999).
4. Ballester, R. *et al.* The NF1 locus encodes a protein functionally related to mammalian GAP and yeast IRA proteins. *Cell* **63**, 851–859 (1990).
5. Martin, G.A. *et al.* The GAP-related domain of the neurofibromatosis type 1 gene product interacts with *ras* p21. *Cell* **63**, 843–849 (1990).

6. Xu, G.F. *et al.* The catalytic domain of the neurofibromatosis type 1 gene product stimulates ras GTPase and complements ira mutants of S. cerevisiae. *Cell* **63**, 835–841(1990).
7. Brannan, C.I. *et al.* Targeted disruption of the neurofibromatosis type-1 gene leads to developmental abnormalities in heart and various neural crest-derived tissues. *Genes Dev.* **8**, 1019–1029 (1994).
8. Jacks, T. *et al.* Tumour predisposition in mice heterozygous for a targeted mutation in *Nf1*. *Nature Genet.* **7**, 353–361 (1994).
9. Silva, A.J. *et al.* A mouse model for learning and memory deficits associated with neurofibromatosis type 1. *Nature Genet.* **15**, 281–284 (1997).
10. Andersen, L.B. *et al.* A conserved alternative splice in the von Recklinghausen neurofibromatosis (NF1) gene produces two neurofibromin isoforms, both of which have GTPase-activating protein activity. *Mol. Cell. Biol.* **13**, 478–495 (1993).
11. Viskochil, D.H. Gene structure and function. in *Neurofibromatosis Type 1: From Genotype to Phenotype* (eds. Upadhyaya, M. & Cooper, D.N.) 39–56 (Bios Scientific Publishers, Oxford, 1998).
12. Zeiher, B.G. *et al.* A mouse model for the delta F508 allele of cystic fibrosis. *J. Clin. Invest.* **96**, 2051–2064 (1995).
13. Hogan, B., Beddington, R., Constantini, F. & Lacy, E. *Manipulating the Mouse Embryo: A Laboratory Manual* (Cold Spring Harbor Laboratory Press, New York, 1994).
14. Huynh, D.P., Nechiporuk, T. & Pulst, S.M. Differential expression and tissue distribution of type I and type II neurofibromins during mouse fetal development. *Dev. Biol.* **161**, 538–551 (1994).
15. Gutmann, D.H., Cole, J.L. & Collins, F.S. Expression of the neurofibromatosis type 1 (NF1) gene during mouse embryonic development. *Prog. Brain Res.* **105**, 327–335 (1995).
16. Nordlund, M.L., Rizvi, T.A., Brannan, C.I. & Ratner, N. Neurofibromin expression and astrogliosis in neurofibromatosis (type I) brains. *J. Neuropath. Exp. Neurol.* **54**, 588–600 (1995).
17. Rizvi, T.A. *et al.* Region-specific astrogliosis in brains of mice heterozygous for mutations in the neurofibromatosis type I (Nf1) tumor suppressor. *Brain Res.* **816**, 111–123 (1999).
18. Cho, Y. & Silva, A.J. Ibotenate lesions of the hippocampus impair spatial learning but not contextual fear conditioning in mice. *Behav. Brain Res.* **98**, 77–87 (1999).
19. Brandeis, R., Brandys, Y. & Yehuda, S. The use of the Morris water maze in the study of memory and learning. *Int. J. Neurosci.* **48**, 29–69 (1989).
20. Gallagher, M., Burwell, R. & Burchinal, M. Severity of spatial impairments in aging: development of a spatial index for performance in the Morris water maze. *Behav. Neurosci.* **107**, 618–626 (1993).
21. Frankland, P.W., Cestari, V., Filipkowski, R.K., McDonald, R.J. & Silva, A.J. The dorsal hippocampus is essential for context discrimination but not for contextual conditioning. *Behav. Neurosci.* **112**, 863–874 (1998).
22. Chen, C. *et al.* Impaired motor coordination correlates with persistent multiple climbing fiber innervation in PKCg mutant mice. *Cell* **83**, 1233–1242 (1995).
23. Barlow, C. *et al. Atm*-deficient mice: a paradigm of ataxia telangietasia. *Cell* **86**, 159–171 (1996).
24. Lijam, N. *et al.* Social interaction and sensimotor gating abnormalities in mice lacking *Dvl1*. *Cell* **90**, 895–905 (1997).
25. Kogan, J.H. *et al.* Spaced training induces normal long-term memory in CREB mutant mice. *Curr. Biol.* **7**, 1–11 (1997).
26. Bunsey, M. & Eichenbaum, H. Selective damage to the hippocampal region blocks long-term retention of a natural and non-spatial stimulus-stimulus association. *Hippocampus* **5**, 546–556 (1995).
27. Upadhyaya, M. & Cooper, D.N. (eds.) *Neurofibromatosis Type 1: From Genotype to Phenotype* (Bios Scientific Publisher, Oxford, 1998).
28. Gutmann, D.H., Zhang, Y. & Hirbe, A. Developmental regulation of a neuron-specific neurofibromatosis type 1 isoform. *Ann. Neurol.* **46**, 777–782 (1999).
29. Klose, A. *et al.* Selective disactivation of neurofibromin GAP activity in neurofibromatosis type 1. *Hum. Mol. Genet.* **7**, 1261–1268 (1998).
30. Atkins, C.M., Selcher, J.C., Petraitis, J.J., Trzaskos, J.M. & Sweatt, J.D. The MAPK cascade is required for mammalian associative learning. *Nature Neurosci.* **1**, 602–609 (1998).
31. Brambrilla, R. *et al.* A role for the Ras signalling pathway in synaptic transmission and long term memory. *Nature* **390**, 281–286 (1997).
32. Largaespada, D.L., Brannan, C.I., Jenkins, N.A. & Copeland, N.G. *Nf1* deficiency causes Ras-mediated granulocyte/macrophage stimulating factor hypersensitivity and chronic myeloid leukemia. *Nature Genet.* **12**, 137–143 (1996).
33. Bollag, G. *et al.* Loss of *Nf1* results in activation of the Ras signalling pathway and leads to aberrant growth in hematopoietic cells. *Nature Genet.* **12**, 144–148 (1996).
34. Metheny, L.J. & Skuse, G.R. NF1 mRNA isoform expression in PC12 cells: modulation by extrinsic factors. *Exp. Cell Res.* **228**, 44–49 (1996).
35. Swiatek, P.J. & Gridley, T. Perinatal lethality and defects in hindbrain development in mice homozygous for a targeted mutation of the zinc finger gene Krox20. *Genes Dev.* **7**, 2071–2084 (1993).
36. Robertson, E.J. Embryo-derived stem cells. in *Teratocarcinomas and Embryonic Stem Cells: A Practical Approach* (ed. Robertson, E.J.) 71–112 (IRL, Oxford, 1987).
37. Laird, P.W. *et al.* Simplified mammalian DNA isolation procedure. *Nucleic Acids Res.* **19**, 4293–4294 (1991).
38. Bourtchuladze, R. *et al.* Deficient long-term memory in mice with a targeted mutation of the cAMP-responsive element-binding protein. *Cell* **79**, 59–68 (1994).